Academic Sciences International Journal of Pharmacy and Pharmaceutical Sciences

ISSN- 0975-1491 Vol 5, Issue 3, 2013

Research Article

COMBINED PEPTIDOMIMETIC AND HIGH THROUGHPUT VIRTUAL SCREENING IDENTIFY NOVEL INHIBITORS OF FASCIN-CATALYZED ACTIN-BUNDLING

OMOTUYI[1,3], I.O., ELEKOFEHINTI[2,3], O.O., EJELONU[3]O.C., KAMDEM JP[2]

[1]Department of Molecular Pharmacology and Neuroscience, Nagasaki University, Japan, [2]Biochemical Toxicology Unit, Universidade Federal de Santa Maria Rs, Brazil, [3]Department of Biochemistry, Adekunle Ajasin University, Akungba-Akoko. Nigeria.
Email: bbis11r104@cc.nagasaki-u.ac.jp

Received: 21 Feb 2013, Revised and Accepted: 25 Mar 2013

ABSTRACT

Objective: Cancer is a disease of complex and multifactorial etiology characterized by unregulated cell division and metastasis. Metastasis is a biophysical event which involves reorganization of extracellular matrix and changes in actin cytoskeletal dynamics leading to the formation of mechanosensoryfilopodia and migratory lamellipodia at the leading edge. Although several proteins are involved in the regulation of actin dynamics, the role played by fascin is unique and its expression has been positively correlated with metastatic cancer phenotypes.

Methods: Combined Peptidomimetic (pepMMsMIMIC) and high throughput virtual screening on MOE platform have been used to screen for fascin inhibitors.

Results: 12 unique aromatic and peptide based compounds have been identified with high affinity for actin-bundling sequence of fascin designated as [29]FGFKVNASASSLKKK[43], H-139 Q-141 S-259 R-383 R-389 based on GBVI/WSA free energy of binding.

Conclusions: These 12 compounds are expected to exhibit potent anticancer activities due to their unique interaction with fascin and ultimately are expected to break new frontiers in the treatment of cancer.

Keywords: Fascin, Anticancer, Novel drug, *In-silico*.

INTRODUCTION

The high morbidity associated with cancer has strong correlation with metastasis [1]. This migration may not be a simple diffusion through plasma or lymph but a complex choreography of biochemical events directed by complex and largely unresolved intracellular and intercellular signaling [2] which dictate cell detachment from primary location and directional migration to secondary tissues [3]. Despite the complexity of the overall process, local actin dynamics-mediated biophysical translocation is clearly observable. This is presented as formation of mechanosensoryfilopodia and migratory lamellipodia at the leading edge [4]. Against this backdrop, research has intensified into deconstructing actin dynamics in normal and cancer cells while the key regulators are emerging[5] as potential pharmacological targets with high promise as cancer chemotherapy [6,7].

Fascin has received significant attention in recent times as a key regulator of cytoskeletal and filopodial actin dynamics. At the leading edge, filopodia comprises bundles of unipolar, formins-nucleated actin filaments with fascin crosslink [8]. In highly motile cancer cells, increased expression of fascin has been observed [9] thus, presenting as a potential target for cancer chemotherapy. However, migrastatin and its analogues are the only widely available inhibitors of fascin [6-7]. Macroketone an analogue of migrastatin inhibits metastasis via interaction with β-trefoil-IV residues of fascin which lies proximal to the two actin-binding sites located within β-trefoil domains I-III [10] [fig 1.1 a, b]. It then becomes imperative to screen the vast majority of chemical library available to find new compounds with the capability of direct and stable interaction with the actin-binding residues of fascin.

In this work, peptidomimetic-based *in silico* screening for chemical compounds with actin-bundling residues of fascin binding fingerprints were queried with compounds from approximately 17million conformers developed from approximately 4 million commercially available chemical collection in MMsINC database using the crystal structure of fascin from the protein-data bank (PDB ID: 3LLP [11,12,13]. The best 400 compounds were retrieved for high throughput virtual screening and scoring analysis using MOE (Molecular Operating Environment 2011.10) platform [14].

METHODS AND MATERIALS

Retrieval of fascin 3d structures and peptidomimetic virtual screening

The three-dimensional structure of human fascin was retrieved from the Protein Data Bank [ID: 3LLP] and uploaded into the pepMMsMIMIC server freely at htpp://mms.dsfarm.unipd.it/pepMMsMIMIC. The structure is managed using the Jmol applet on the server. The residues selected for peptidomimetic query were previously identified as either fascin actin-bundling residues (29FGFKVNASASSLKKK43)[5] or proximal to these domain (H-139 Q-141 S-259 R-383 R-389) [8]. The scoring method selected for this analysis is fingerprint-based filtering of shape similarity. A total of 400 unique compounds were retrieved ranked according to their fingerprint similarity which is estimated by weighted similarity index Sw[15].

Docking simulation on MOE platform

Flexible ligand-docking was performed using MOE (molecular operating environment, 2011.10) platform[14]. The 3D of fascin used in pepMMsMIMIC server for peptidomimetic screening was uploaded into the MOE for high throughput virtual screening and pose scoring. Water molecules and other non-amino acid component were removed followed by 3D protonation and parametization using the protein preparation pull-down menu, all the missing atoms, incorrect bond stretch and length were corrected. The LigX menu was used to tether heavy atoms and recheck the parameters before docking. The docking simulation was done using the following protocols: Poses were generated using triangle matcher placement[14]. Receptor + solvent mode was assigned to the receptor while the ligand (site) is defaulted to bind on selected residues including 29FGFKVNASASSLKKK43[5], H-139 Q-141 S-259 R-383 and R-389[8]. The first scoring was estimated using London dG defined by the equation below:

$$\Delta G = c + E_{flex} + \sum_{h-bonds} c_{HB} f_{HB} + \sum_{m-lig} c_M f_M + \sum_{atoms\ i} \Delta D_i$$

$$\Delta D_i = c_i R_i^3 \left\{ \iiint_{u \notin A \cup B} |u|^{-6}\, du - \iiint_{u \notin B} |u|^{-6}\, du \right\}$$ [12]

D_i is the desolavation energy, c represents the average gain/loss of rotational and translational entropy, E_{flex} is the energy due to loss of flexibility of the ligand. F_{HB} measures geometric imperfections of hydrogen bonds. C_{HB} is the energy of an ideal hydrogen bond, Fm measures geometric imperfections of metal ligation,Cm is the energy of an ideal metal ligation. A and B are protein and/or ligand volumes with atoms *i belonging to volume B; R_i is the salvation radius of atom i. C_i is the desolavation coefficient of atom i.*

Each pose was refined by forcefield and subsequently rescored using the GBVI/WSA dG function as defined below:

$$\Delta G \approx c + \alpha \left[\frac{2}{3}(\Delta E_{coul} + \Delta E_{sol}) + \Delta E_{vdw} + \beta \Delta SA_{weighted} \right] \quad [14]$$

C represents the average gain/loss of rotational and translational entropy, α is forcefield-dependent constant, E_{coul} is the coulombic electrostatic term, E sol is the salvation electrostatic term, E_{vdw} is the van der Waals contribution to binding and $SA_{weighted}$ is the surface area weighted by exposure. The veracity of GBVI/WSA dG as scoring function has been validated by [16]. The 2D depiction of the protein-ligand complex has been reported by[17].

PYMOL (Delano Scientific LLC, USA) was used for surface map visualization for ligand and receptor interaction. The names of the compounds were retrieved using MMscode from MMsINC database (www.mms.dsfarm.unipd/it/MMsINC/search/) and pubchem database (www.pubchem.ncbi.nlm.gov).

RESULTS

Identification of novel fascin-catalysed actin-bundling inhibitors

pepMMsMIMIC a web-oriented peptidomimetic compound virtual screening was used to identify 400 unique compounds (data not shown) from the list of 17million conformers developed from approximately 4 million commercially available chemical collection in MMsINC database using the 3D structure of fascin obtained from the protein databank (3LLP) and fingerprint-based filtering of shale similarity of H-139 Q-141 S-259 R-383 R-389 representing the conserved residues proximal to the putative actin-binding site of fascin-1 [8] and 29FGFKVNASASSLKKK43 (fig 1.1 a,b) which is the structural motif for the actin bundling activity and fascin regulation via ser39 phosphorylation by PKC [5]. This screening method generates best five lowest-energy confomers using Rotate ver. 1.0 software and subsequently docking these compounds into the pockets of the proteins using defined pharamcophoric features such as the tryptophan, histidine and tyrosine side chains, hydrogen-bond donor/acceptor, negatively and positively ionizable groups, aromatic and hydrophobic features. Finally, the binding is scored in order of their weighted similarity index Sw [18]. To isolate the compounds with exceptional binding affinity for Fascin, the 400 compounds retrieved from the pepMMsMIMIC webserver were imported to our MOE database for docking and rescoring. The receptor is prepared by removal of water molecules and extra chain present, followed by protonation and parametization. The receptor for docking on MOE was defined as receptor+solventwhile the site atoms were defined as selected residues similar to the residues used for initial screening. Poses were generated by aligning ligand triplet of atoms on triplet of alpha spheres as described in triangle matcher mode in MOE in each pose generated, the London dG scoring function was first used to estimate the free energy of binding. While forcefield refinement scheme was used which is more accurate than the GridMin but computationally more expensive. Finally, post refinement rescoring was done by GBVI/WSA dG which takes into cognizance of the contribution of columbic electrostatic term, solvation electrostatic term, van der Waals contribution and surface weighted by exposure [14,19]. The combination of these methods is highly predicted to yield a robust dataset of compounds exhibiting specific interaction with actin-bundling residues of fascin. Furthermore, we predefined -9.0kcal/mol as the cutoff binding energy this step ultimately identified 12 of the starting 400 compounds as exhibiting high affinity for the actin-bundling domain of fascin (figure1.0). The free energy of binding and features of the compounds are shown on table 1.0. It must be understood that efforts have been made towards establishing a correlation between the free energy of binding and IC-50 of compounds [20]. This mathematical relationship strongly indicates low IC-50 values positively correlate with low free energy of binding; we therefore speculate that these compounds will have low IC-50 during wet screening experiments.

Deconstructing the fascin-binding pattern of individual compounds

Taking advantage of the presentation of protein-ligand complex in 2D format available on MOE [17] we provide an information-rich 2D interaction between the actin-bundling domain of fascin and selected compounds [17]. The diagrams well accentuate the hydrogen bonds, contours, solvent exposure, covalent interactions and the contribution of pi-cloud of electrons. The interaction between MMs02455752 and actin-bundling region of fascin is shown in Fig. (2.0). This compound is 6-methoxy-3chloro 9-amino substituted acridine rings joined by an octane1,8-diamine chain. The interaction is largely driven by hydrogen bonding interaction between the electron withdrawing effect of chlorine atoms on hydroxyl group hydrogen of ser409, and carboxyl-amido hydrogen of glu142 and the pi-electron density of acridine heterocyclic ring which interacts with the imidazole cation of his392 and the e-amino nitrogen of Lys-42. Visibly, the cationic centers of the basic amino acids (histidine-392 and lysine-42) well interact with the electron-rich heterocyclic aromatic center of acridine thus, accounting for a total of -2.0kcal/mol of energy while chlorine-mediated hydrogen bond accounts for -2.2kcal/mol. Although, bis-acridines have been used in the management of cancer, prion accumulation and microbial infections, the underlying mechanisms have been linked to DNA-acridine adduct formation [21]. This study may have provided a unique and new insight into the full complement of bis-acridines anti-cancer bioactivity.

MMs03916843 structure is built on di-p-butyoxy m-methylaminobromo-benzene linked by glutamido chain. Hydrogen bonding interaction and pi-electrons are responsible for the stabilization of the interaction. The N-N linkage between of the methyl-amino group and the glutamido-nitrogen interacts with glutamine 13 with an energy of -4.1 kcal/mol while the phenyl ring pi-electrons interacts with the cationic center of e-amino group of lysine 460 with energetic value of -0.6kcal/mol. The flexibility of the carbon- carbon bond allows spatial occupation of this compound into the actin-bundling pocket proximal to the reactive residues as shown by the contour scheme (fig 2.1). This compound is only found in ZINC database so possibly newly developed without any known bioactivity. However, some alky-haloaryl-derivatized compounds have been identified as antitumour agents with which MMs03916843 share structural similarity [22].

Hydrogen-bonding interaction between the partially charged oxygen atom of the oxoacetyl substituent of benzothiopene-3-carboxylate and cationic center of the guanidino group of arg389 is the stabilizing force between MMs-03115720 and fascin (fig 2.2). Although, hydrogen bonding accounts for -6.3kcal/mol, nitrogen-nitrogen single bond between the hydrazinyl bridge constitute a central flexible diazine unit which may play important role in correctly localizing this compound into similar contour within actin-bundling residues of fascin and may further drive stability of the complex [23]. Similarly, a quantitative structure-activity relationship (QSAR) study has identified benzothipene derivatives as potent anticancer agents [24] and the mechanism has been linked to histone deacetylase inhibition. In a related study, other groups have identified the anticancer mechanism as due to DNA-binding and topoisomoreases I and II inhibition [25].

MMs02458931 is structurally analogous to MMs02455724 but unlike the later, it only has 3- methyl substituents on the two acridine rings. As expected, absence of chlorine blanks out the contribution of hydrogen bonding but the pi-electron contribution is preserved. The fused acridine heterocyclic aromatic rings proximal to His392 and lys42 donate pi-electron density which spatially interacts with imidazole cationic center histidine 392 and e-amino nitrogen center of lysine 42 (fig 2.3). The total energies for this

interaction is -2.1kcal/mol. As this compound is in the class of bis-acridines, their anti-cancer properties have been previously exploited [21].

MMs02185018 has two substituted 1,3,5-triazin moieties bridged by cyanophenyl-group. Although, one of the triazin and its substituents are exposed, the cyanophenyl bridge and the second triazin residues are more buried into the actin-bundling domain of fascin. These buried moieties interact with Lys41 and His392 via pi-electron density (fig 2.4). The inflexibility of carbon-carbon bond between triazin C-5 and cyanophenyl groups may play significant role on exposing the dimethylbutanoylamino moieties.

MMs02460092 shares structural similarities with MMs02455724 and MMs0245893 whose anticancer potencies have been discussed previously. However, the defining features of MMs02460092 include: an hexanediamine bridge rather than octane1,8-diamine bridge in the previous molecules (fig 1.0). It also has a unique 3-propoxyl group. The heterocyclic acridine ring proximal to Lys41 interacts with this residue using pi-electrons (fig 2.5).

Fig (2.6) shows the interaction between fascin and MMs03924089; a di-1,3-dioxoisoindol-2-oyl ethoxyl-ethyl derivative of 1,4,10,13-tetraoxa-7-16-diazacyclooctadecane. While the 1,4,10,13-tetraoxa-7,16-diazacyclooctadecane moiety has observable interaction with fascin residues, the isoindole-1,3-dione substituents effectively participate in hydrogen bonding with Arg389. The isoindole rings also offers pi-electrons for interaction with Gly393 and His392 with a total energy of -5.4kcal/mol. previously, phenyl-isoindole derivatives have been classified as anticancer agents due to their cytotoxicity [26] and in some experiments, chaperone protein Hsp90 inhibition.

MMs03919433 has been previously recognized as collagenase substrate in the quantitative determination of collagenase (Fluka 27637). It is a peptide mimic containing phenyl-Gly-Pro-Gly-Pro-Ala-OH. This structural uniqueness is observed in the recognition and binding pattern with fascin. First, the flexibility of the inter-residue bond allows for closer packing into the actin-bundling domain of fascin with consequent few exposed atoms. Secondly, the ligand residues make specific contact with the residues of fascin allowing for establishment of hydrogen bonding interaction with fairly high negative energies (fig 2.7). Specific hydrogen bonding interactions are made with Gln13 (-2.4kcal/mol), Gly390 (-2.0kcal/mol) Gln11 (-1.4kcal/mol) and Arg389 (-1.0kcal/mol) pi-electron of phenylglycinamide group also interacts with e-amino cation of Lys460 contributing an energy of -0.7kcal/mol. The use of peptides as novel class of anticancer drugs has been given priority in recent times [27] and MMs03919433 may emerge as the newest in the list.

In Fig. (2.8) the interaction between MMs03128586 and fascin is shown. The ligand is built on benzoyloxyphenyl-methyldienehydrazinyl structures joined together by 1,7-heptadioic moiety. The flexibility of the 1,7-heptadioic moiety is largey responsible for placement of the two benzoyloxyphenyl-methydienehydrazinyl groups into the actin-bundling domain of fascin with consequent formation of hydrogen bonding interaction between the amido oxygen of heptadioic moiety and Arg389 which accounts for -3.8kcal/mol of energy. The anticancer potency of benzyl-benzoate the core component of MMs03128586 may not have been reported but its antiparasitic activity is well known [28]. It is also a major composition of the essential oils of *Kaempferia rotunda* L. and *Kaempferiaangustifolia* Roscoe rhizomes from Indonesia used as insecticidal ethnopharmacotherapeutic agent[29].MMs02456592 is an isomer of MMs 02455724, the only structural difference is the location of the 2-methoxyl substituent on carbon-2 of the acridine ring in the former while it is on carbon-6 in the later. This alteration has very subtle effect on residue recognition and binding of MMs02456592; in that the distance between His393 and the proximal acridine ring is slightly longer (3.96 and 4.62 angstrom) (fig 2.9) compared with MMs02455724 (3.95 and 4.33 angstrom, fig 2.1). It may be oversimplifying to state that this physical restraint is responsible for the loss of chlorine interaction as with ser409 and gln141 as observed for MMs02455724 but it certainly does play responsible for the free energy of binding difference 568.3kcal/mol (table 1.0).

Fig. 3.0 shows another structural analogue of MMs024557240; in this structure (MMs02462072), 6-chloro group is absent in the acridine ring. The binding of this analogue is principally via pi-electron to His392 and Gly393 with observed weaker free energy of binding to fascin compared to the previous ones.

MMs02374885 is di-1,4-dihydroindeno1,2-pyrole-3-carboxylic acid linked together by amino-propyl-methyl amino-propylamine chain. The interaction with actin bundling domain of fascin is driven by hydrogen bonding interaction between fascin Glu8 carboxylic acid and pyrrole nitrogen of dihydroindenol-pyrrole-3-carboxamide, between carboxamide oxygen of ligand and Arg389 and pi-electron between dihydroindenol moiety and Lys41 (fig 3.1).

Table 1.0: High affinity fascin binding inhibitors and their corresponding free energies

pepMMs-code	Name	Formula	Mw(g/mo)l	dG (kcal/mol)
MMs02455724	N,N'-bis(3-chloro-6-methoxyacridin-9-yl)octane-1,8-diamine	$C_{36}H_{36}C_{l2}N_4O_2$	627.60264	-9.6080
MMs03916843	*N,N'-bis[(5-bromo-2-butoxy-phenyl)methyleneamino] pentanediamide*	$C_{27}H_{34}Br_2N_4O_4$	638.401	-9.5964
MMs03115720	ethyl 2-[[2-[(2E)-2-[(4-benzoyloxy-3-ethoxyphenyl)methylidene]hydrazinyl]-2- oxoacetyl]amino]-4,5,6,7-tetrahydro-1-benzothiophene-3-carboxylate	:$C_{29}H_{29}N_3O_7S$	563.62146	-9.5848
MMs02458931	N,N'-bis(3-methylacridin-9-yl)octane-1,8-diamine	$C_{36}H_{38}N_4$	526.71372	-9.2423
MMs02185018	N-[4-[3-[4,6-bis(3,3-dimethylbutanoylamino)-1,3,5-triazin-2-yl]-5-cyanophenyl]-6-(3,3-dimethylbutanoylamino)-1,3,5-triazin-2-yl]-3,3-dimethylbutanamide	$C_{37}H_{51}N_{11}O_4$	713.87214	-9.2299
MMs02460092	N,N'-bis(3-propoxyacridin-9-yl)hexane-1,6-diamine	$C_{38}H_{42}N_4O_2$	586.76568	-9.2239
MMs03924089	2-[2-[2-[16-[2-[2-(1,3-dioxoisoindol-2-yl)ethoxy]ethyl]-1,4,10,13-tetraoxa-7,16-diazacyclooctadec-7-yl]ethoxy]ethyl]isoindole-1,3-dione	$C_{36}H_{48}N_4O_{10}$	696.78712	-9.2107
MMs03919433	phenyl-Gly-Pro-Gly-Gly-Pro-Ala-OH	$C_{27}H_{36}N_6O_9$	588.60954	-9.1860
MMs03128586	[2-[[[7-[(2E)-2-[(2-benzoyloxyphenyl)methylidene]hydrazinyl]-7-oxoheptanoyl]hydrazinylidene]methyl]phenyl] benzoate	$C_{35}H_{32}N_4O_6$	604.65178	-9.1457
MMs02456592	N,N'-bis(6-chloro-2-methoxyacridin-9-yl)octane-1,8-diamine	$C_{36}H_{36}C_{l2}N_4O_2$	627.60264	-9.0397
MMs02462072	N,N'-bis(3-methoxyacridin-9-yl)octane-1,8-diamine	$C_{36}H_{38}N_4O_2$	558.71252	-9.0353
MMs02374885	N-[3-[3-(1,4-dihydroindeno[1,2-b]pyrrole-3-carbonylamino)propyl-methylamino]propyl]-1,4-dihydroindeno[1,2-b]pyrrole-3-carboxamide	$C_{31}H_{33}N_5O_2$	507.62602	-9.0100

dG (GBVI/WSA dG)

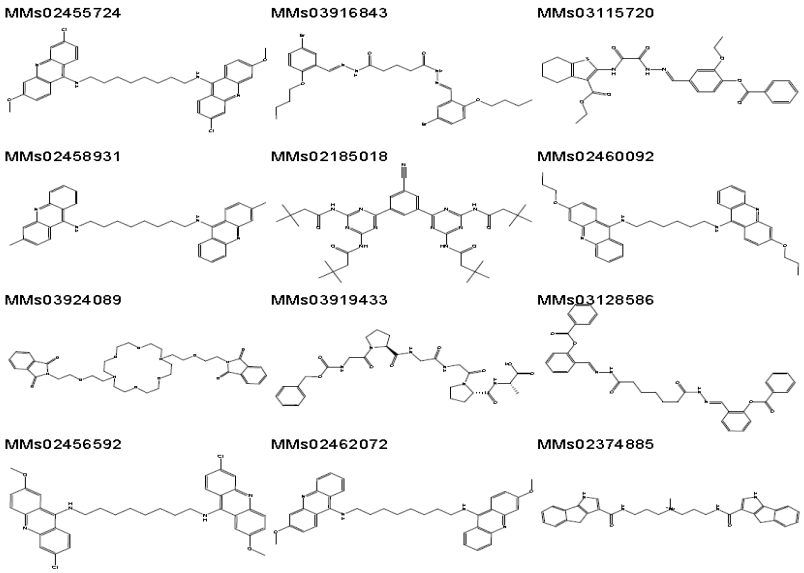

Fig. 1.0: Collection of 12 compunds with high affinity for actin-bundling domain of fascin.

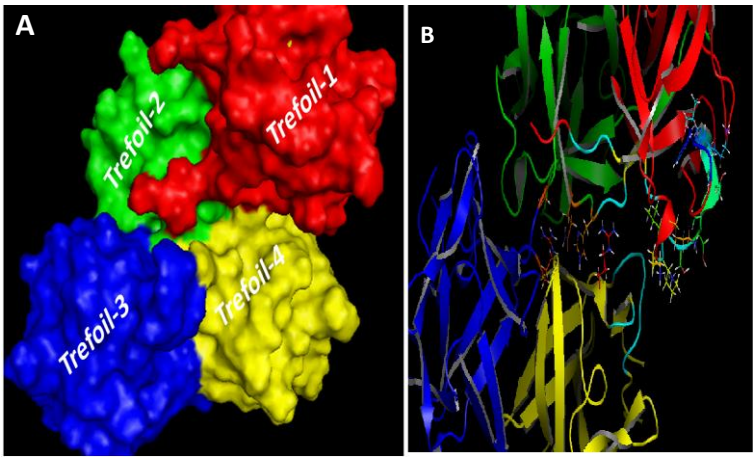

Fig. 1.1: fascin-1 3D structure a) shows the different trefoil domains of fascin-1; trefoil-1 (red), trefoil 2 (green), trefoil 3 (blue) and trefoil 4 (yellow) b) cartoon representation of fascin trefoils with side chain depicting actin-bundling residues (^{29}FGFKVNASASSLKKK ^{43}) and proximal residues H-139 Q-141 S-259 R-383 R-389.

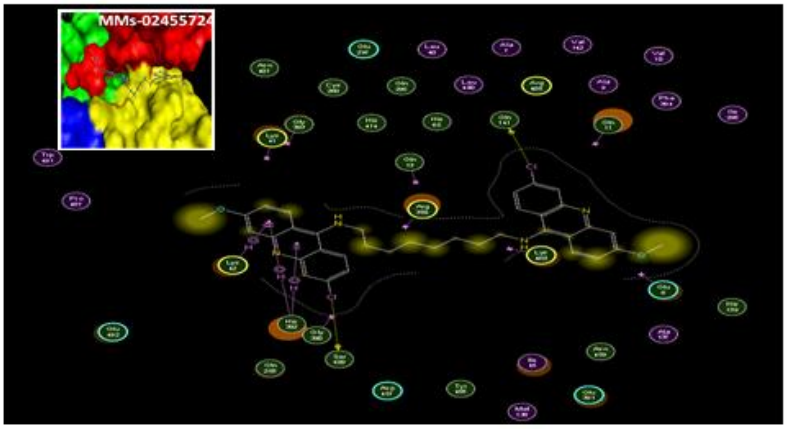

Ligand		Receptor			Interaction	Distance	E (kcal/mol)
CL 39	O	SER 409	(A)		H-donor	3.36	-1.5
CL 42	O	GLN 141	(A)		H-donor	3.84	-0.7
6-ring	CB	LYS 42	(A)		pi-H	4.06	-0.6
6-ring	CA	HIS 392	(A)		pi-H	3.95	-0.7
6-ring	CA	HIS 392	(A)		pi-H	4.33	-0.7

Fig. 2.0 Surface diagram (upper right) and 2D depiction for the interaction of MMs02455724 with fascin actin-bundling residues. (bottom right) The designation of binding residues, interaction type and bond energies.

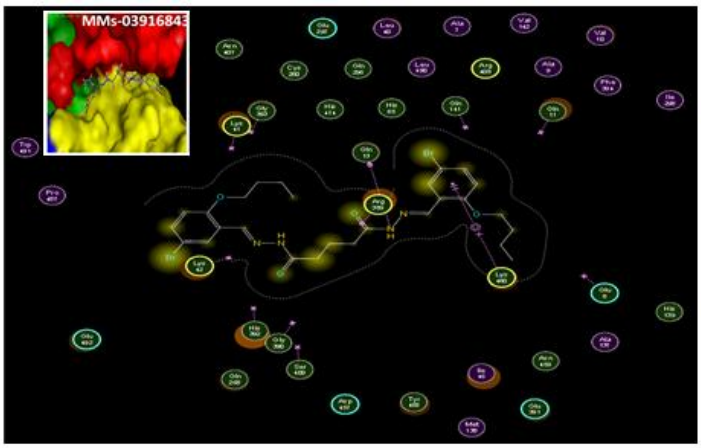

Ligand		Receptor			Interaction	Distance	E (kcal/mol)
N 22	OE1	GLN 13	(A)		H-donor	3.03	-4.1
6-ring	NZ	LYS 460	(A)		pi-cation	4.43	-0.6

Fig. 2.1: Surface diagram (upper right) and 2D depiction for the interaction of MMs03916843 with fascin actin-bundling residues. (bottom right) The designation of binding residues, interaction type and bond energies.

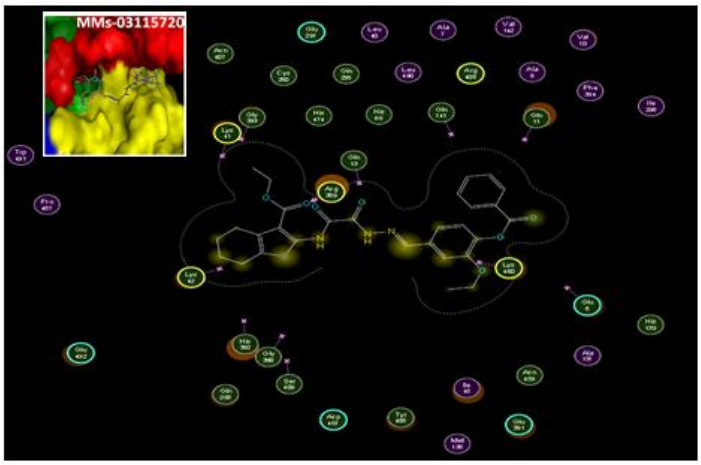

Ligand		Receptor			Interaction	Distance	E (kcal/mol)
O 37	NH2	ARG 389	(A)		H-acceptor	2.86	-6.3

Fig 2.2 Surface diagram (upper right) and 2D depiction for the interaction of MMs03115720 with fascin actin-bundling residues. (bottom right) The designation of binding residues, interaction type and bond energies.

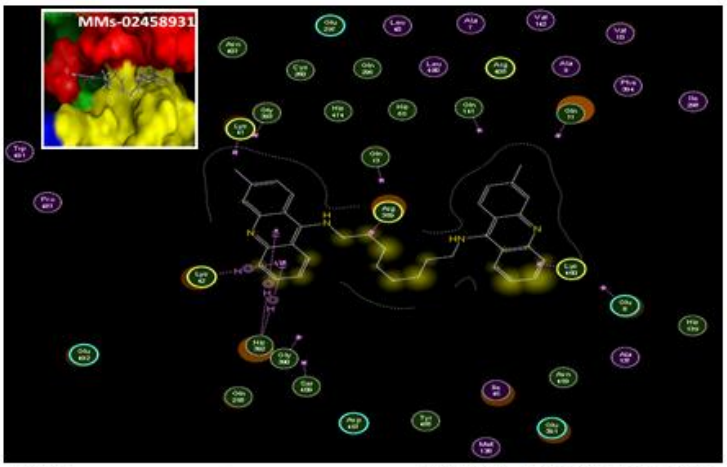

Ligand		Receptor			Interaction	Distance	E (kcal/mol)
6-ring	CB	LYS 42	(A)		pi-H	4.08	-0.7
6-ring	CA	HIS 392	(A)		pi-H	4.03	-0.7
6-ring	CA	HIS 392	(A)		pi-H	4.34	-0.7

Fig. 2.3: Surface diagram (upper right) and 2D depiction for the interaction of MMs02458931 with fascin actin-bundling residues. (bottom right) The designation of binding residues, interaction type and bond energies.

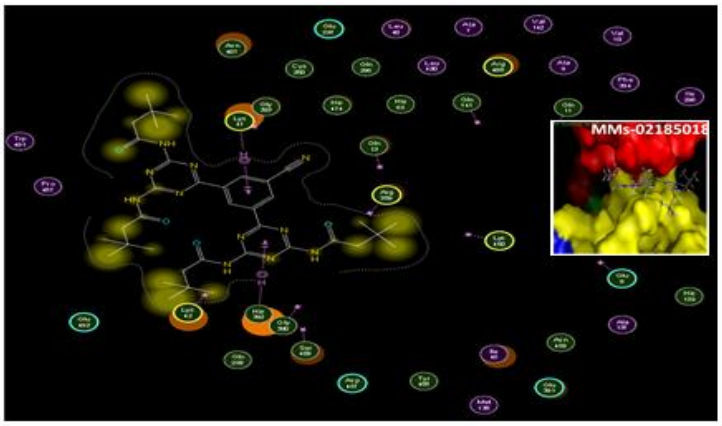

Ligand		Receptor			Interaction	Distance	E (kcal/mol)
6-ring	CA	LYS 41	(A)		pi-H	4.30	-0.7
6-ring	CA	HIS 392	(A)		pi-H	4.38	-0.6

Fig. 2.4: Surface diagram (upper left) and 2D depiction for the interaction of MMs02185018 with fascin actin-bundling residues. (bottom right) The designation of binding residues, interaction type and bond energies.

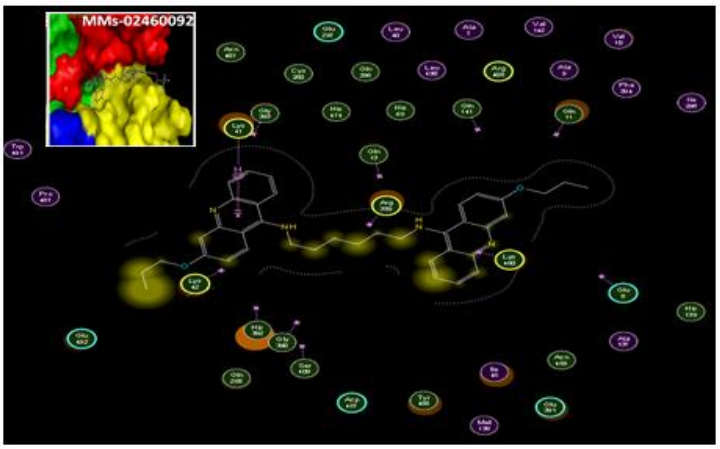

Ligand		Receptor			Interaction	Distance	E (kcal/mol)
6-ring	CA	LYS 41	(A)		pi-H	4.66	-0.6

Fig. 2.5: Surface diagram (upper right) and 2D depiction for the interaction of MMs02460092 with fascin actin-bundling residues. (bottom right) The designation of binding residues, interaction type and bond energies.

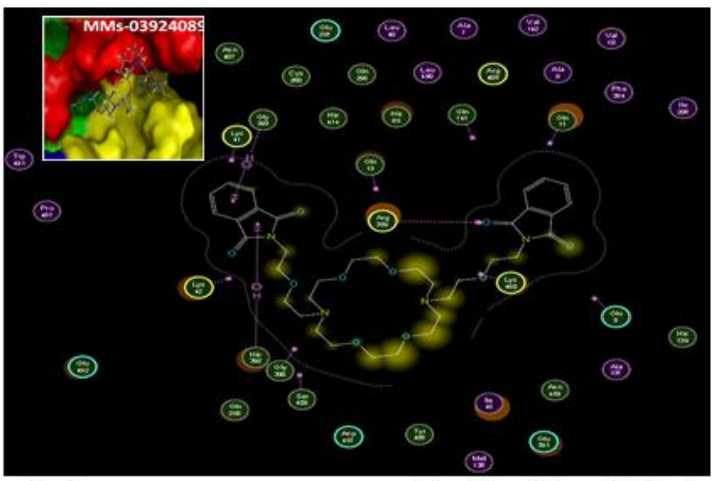

Ligand		Receptor			Interaction	Distance	E (kcal/mol)
O 40	NH1	ARG 389	(A)		H-acceptor	2.84	-3.7
5-ring	CA	HIS 392	(A)		pi-H	4.21	-0.9
6-ring	CA	GLY 393	(A)		pi-H	3.68	-0.6

Fig. 2.6: Surface diagram (upper right) and 2D depiction for the interaction of MMs03924089 with fascin actin-bundling residues. (bottom right) The designation of binding residues, interaction type and bond energies.

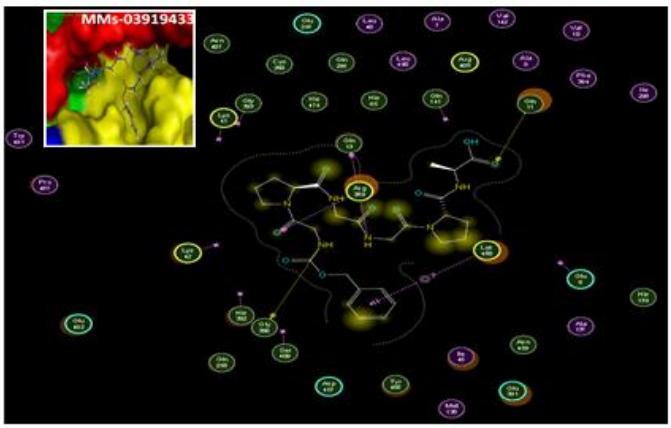

Ligand			Receptor			Interaction	Distance	E (kcal/mol)
N	18	OE1	GLN 13	(A)		H-donor	3.03	-2.4
N	34	O	GLY 390	(A)		H-donor	2.87	-2.0
O	5	N	GLN 11	(A)		H-acceptor	3.00	-1.4
O	32	NE	ARG 389	(A)		H-acceptor	3.29	-1.0
6-ring		NZ	LYS 460	(A)		pi-cation	3.32	-0.7

Fig. 2.7: Surface diagram (upper right) and 2D depiction for the interaction of MMs03919433 with fascin actin-bundling residues. (bottom right) The designation of binding residues, interaction type and bond energies.

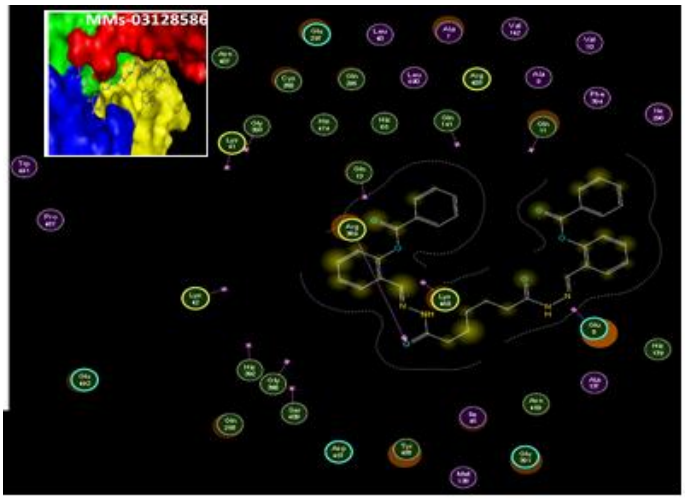

Ligand			Receptor			Interaction	Distance	E (kcal/mol)
O	27	NH1	ARG 389	(A)		H-acceptor	3.00	-3.8

Fig. 2.8: Surface diagram (upper right) and 2D depiction for the interaction of MMs03128586 with fascin actin-bundling residues. (bottom right) The designation of binding residues, interaction type and bond energies.

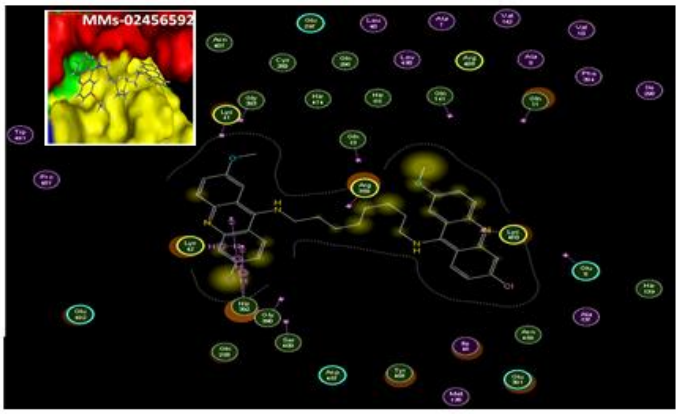

Ligand		Receptor			Interaction	Distance	E (kcal/mol)
6-ring	CB	LYS 42	(A)		pi-H	3.92	-0.6
6-ring	CA	HIS 392	(A)		pi-H	3.96	-0.8
6-ring	CA	HIS 392	(A)		pi-H	4.62	-0.7

Fig. 2.9: Surface diagram (upper right) and 2D depiction for the interaction of MMs02456592 with fascin actin-bundling residues. (bottom right) The designation of binding residues, interaction type and bond energies.

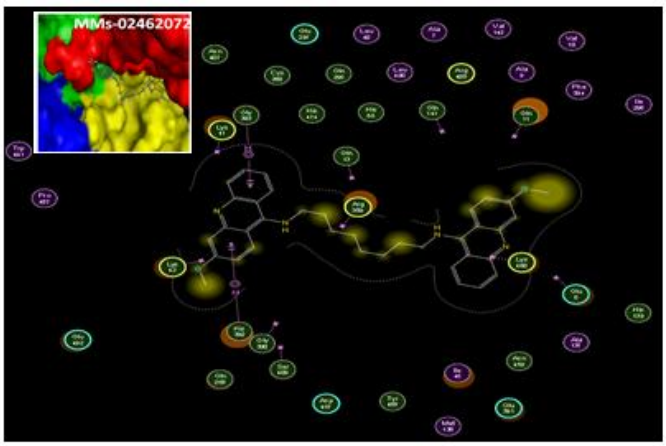

Ligand		Receptor			Interaction	Distance	E (kcal/mol)
6-ring	CA	HIS 392	(A)		pi-H	3.86	-0.6
6-ring	CA	GLY 393	(A)		pi-H	3.66	-0.9

Fig. 3.0: Surface diagram (upper right) and 2D depiction for the interaction of MMs02462072 with fascin actin-bundling residues. (bottom right) The designation of binding residues, interaction type and bond energies.

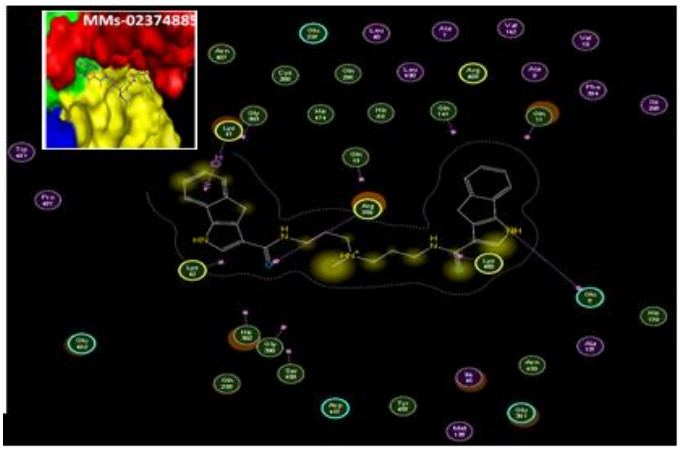

Ligand			Receptor			Interaction	Distance	E (kcal/mol)
N	10	OE1	GLU 8		(A)	H-donor	3.53	-1.3
O	26	NE	ARG 389		(A)	H-acceptor	3.11	-3.6
O	26	NH2	ARG 389		(A)	H-acceptor	3.15	-3.0
6-ring		CG	LYS 41		(A)	pi-H	3.95	-0.9

Fig. 3.1: Surface diagram (upper right) and 2D depiction for the interaction of MMs02374885 with fascin actin-bundling residues. (bottom right) The designation of binding residues, interaction type and bond energies.

DISCUSSION

Global cancer epidemiological statistics reveal that cancer is the leading cause of death and second leading cause of death in economically developed and developing countries according to 2008 estimates [30]. This statistics has engendered intensive research into the mechanism of cancer pathogenesis but the more insight we gain into these mechanisms, the more complex it becomes to find a cure to cancer [31]. First, cancer cells share almost similar transduction pathways with normal cells [32,33,34], they become immune evasive phenotypes [35] and develop mechanisms for therapeutic compound efflux through ABC transporters [36] and increased expression of broad-range of detoxifying enzymes [36] thereby eliminating selective toxicity of therapeutic compounds, evading immuno-surveillance mechanisms and de-accumulation of therapeutic compounds. One property that seems restricted to few normal cells but exhibited by all cancer cells and immune cells is migration [31]. Our understanding of this biophysical event has been beneficial to the development of therapeutics agents for cancer management. Migrastatin [7] together with their analogues were developed on the principle of migration inhibition in cancer cells [8]. The atomic details of the interaction between macroketone and fascin target is well understood and the data show that macroketone interacts with β-trefoil IV residues while fascin-mediated actin-bundling principally occurs within β-trefoil I and III[5]. It has been presented that ser39 in the β-trefoil I exists within the spatial crevice of macroketone binding and the protein kinase C-mediated phosphorylation of this serine residue is associated with loss of actin bundling functions[35]. It is logically inconsistent to assume that inhibition of serine39 phosphorylation by protein kinase C (PKC) has significant contribution to macroketone bioactivity as inhibition of phosphorylation will correlate with increased F-actin bundling [9]. The proximity of macroketone binding to the 29-FGFKVNASASSLKKK-43 motif may be responsible for actin-bundling inhibitory action [5]. But our data still suggest the presence of glycerol in this groove may further serve to enhance the stability of the interaction as the free energy of binding recorded is relatively high (data not shown).

In contrast to the binding pattern of macroketone, we have targeted the fascin residues involved in acting bundling activity and we have identified 12 compounds out of approximately 17 million compounds available in the MMsINC database exhibiting high affinity to the actin-bundling residues. Out of the 12 compounds, five (5) belongs to the bis-acridine family. Anticancer potency of bis-acridine has been documented [21]. Here, we present fascin

inhibition as a new mechanism for bis-acridine-anticancer properties different from their adduct formation with DNA[36]. The high affinity of bis-acridine-based compounds to the actin-bundling domains has been shown to involve pi-electron center of their heterocyclic aromatic rings and the cationic surface of fascin-bundling domains which is rich in basic amino acids such as Lys and His residues. Same argument holds for the rest of the compounds as they are derivatives of aromatic or heterocyclic aromatics compounds such as alkyoxy-halobenzenes (MMs03916843), benzothiophene (MMs03115720), 1, 3, 5-triazin-2yl-5-cyanobenzene (MMs02185018), dioxoisoindole (MMs03924089), benzyl benzoate (MMs03128586) and phenylduhdroindenol-pyrole (MMs02374885). We also discovered a peptide-based compound used as reagent in qualitative determination of collagenase activity (MMs03919433) this compounds further raises the possibility of peptide based anticancer agent which has been given some considerations in recent times [28].

CONCLUSION

Fascin is widely reputed as a biomarker for metastatic tumour, this is due to increased gene expression and this expression pattern correlates well with cancer migration and worse disease outcome and higher morbidity. Migrastatin and its analogues have been widely used as cancer chemotherapeutics on the principle of fascin inhibition. We have discovered 12 new classes of compounds with high affinity for the F actin-bundling residues of fascin. These compounds are essentially aromatic in structure forming highly stable complexes from electrostatic interaction between the electron rich pi-cloud of electron on the aromatic moieties and highly cationic centers of actin-bundling residues of fascin contributed by rich lysine and histidine residues. With these new compounds, we expect oncologists and pharmaceutical companies to explore them as anticancer agents with the ultimate hope that cancer mortalities be significantly reduced.

REFERENCES

1. Hanahan D, Weinberg RA The hallmarks of cancer. Cell 2000; 100: 57–70.
2. Fidler IJ The pathogenesis of cancer metastasis: the 'seed and soil' hypothesis revisited. Nat Rev Cancer 2003; 3: 453–458.
3. Wels J, Kaplan RN,Rafii S,Lyden D Migratory neighbors and distant invaders: tumor-associated niche cells. Genes Dev2008; 22: 559–574.
4. Le Clainche C,Carlier MF Regulation of actin assembly associated with protrusion and adhesion in cell migration. PhysiologiReviw 2008; 88: 489-513.
5. Jansen S, Collins A, Yang C,Rebowski G,Svitkina T, Dominguez R Mechanism of actin filament bundling by fascin. J BiologicaChem 2011; 286: 30087-30096.
6. Gaul C,Njardarson JT, Shan D, Dorn DC, Wu KD, Tong WP, Huang XY The migrastatin family: discovery of potent cell migration inhibitors by chemical synthesis. J AmeChem Society2004; 126: 11326-11337.
7. Anquetin G,Horgan G,Rawe S, Murray D, Madden A,MacMathuna P, Doran PSynthesis of Novel Macrolactam and Macroketone Analogues of MigrastatinfromD-Glucal and Comparison with Macrolactone and Acyclic Analogues: A Dorrigocin A Congener Is a Potent Inhibitor of Gastric Cancer Cell Migration. Eur J Organic Chem2008; 11: 1953-1958.
8. Sedeh RS,Fedorov AA,Fedorov EV, Ono S, Matsumura F,Almo SC,et al. Structure, evolutionary conservation, and conformational dynamics of Homo sapiens fascin-1, an F-actin crosslinking protein. J MolBiol 2010; 400: 589–604.
9. Grothey A,Hashizume R,Sahin A, McCrea PD Fascin, an actin-bundling protein associated with cell motility, is upregulated in hormone receptor negative breast cancer. Bri J Cancer 2000; 83: 870–873.
10. Dias LC,Finelli FG,Conegero LS, Krogh R,Andricopulo AD Synthesis of the Macrolactone of Migrastatin and Analogues with Potent Cell-Migration Inhibitory Activity. Eur J Organic Chem2010; 35: 6748-6759. doi: 10.1111/j.1747-0285.2012.01442.
11. Chen L, Yang S,Jankovic J, Zhang J, Huang XY Migrastatin analogues target Fascin to block metastasis. Natur2010; 464: 1062-6.
12. Parida P, Yadav R, Shanker B, Charkraborty DP, Das A, Singh NK *In-silico* protein ligand interaction study of typical antipsychotic drugs against dopaminergic D2 receptor. Int J Pharm and pharmceusci 2012; 5: 183-189.
13. Nerkar AG, Joshi PP, Mohite S, Singh S, More MA, Chikhale HU, Sawant SD *In-silico* design, synthesis and pharmacological screening of novel mono and di-bromoquinazolinonederivatives as NMDA receptor antagonists for anticonvulsant activity. Int J Pharm and pharmceusci 2012; 5: 331-335.
14. Molecular Operating Environment (MOE) Chemical Computing Group Inc., 1010 Sherbooke St. West, Suite #910, Montreal, QC, Canada, H3A 2R7, 2011.
15. Floris M,Masciocchi J,Fantom M, Moro S Swimming into peptidomimetics chemical space using pepMMsMIMIC. Nucl Acids Res2011; W: 261-269.
16. CorbeilCR, Williams CI,Labute P Variability in docking success rates due to dataset preparation. J Comput Aided Mol Des2012; 26: 775-86.DOI: 10.1007/s10822-012-9570-1.
17. Clark AM,Labute P Depiction of protein-Ligand Complexes. J ChemInf Model2007; 47: 1933-1944.
18. Babu AP,Chitti S, Rajesh B,Prasanth VV,Radha JV,Khadar R In silico ligand design and docking studies of GSK-3β inhibitors. Chem-bio informatics Jour2010; 10: 1-12.
19. Gamage SA, Spicer JA, Atwell GJ, Finlay GL,Baguley BC, Denny WAJ Med. Chem1999; 42: 2383-2393.
20. Ates-Alagoz Z, Coleman N, MartinM, Wan A,Adejare A Syntheses and *In Vitro* Anticancer Properties of Novel Radiosensitizers.ChemBiol Drug Des2012; 80: 853-61.doi: 10.1111/j.1747-0285.2012.01442.
21. Datta A,Revaprasadu NIsolation of bis(1,4-diphenyl-1,4-bis(2-pyridyl)-2,3-diaza- 1,3-butadiene) disilver with bridging (n-n) dinucleating subunits: formation of a 6-membered chelate ring. Turk J Chem2010; 34: 277 – 284.
22. Satish K,Sarankar KT,Jitendra B,Parul M,Pathak AK,Mukul TQSAR Study of Novel Benzothiophene Derivatives as Potent Anticancer Agent. Int J AdvPharmaceuSci2010; 1: 309-318.
23. Aleksić M, Bertoša B,Nhili R,Uzelac L, Jarak I, Depauw S, et al.Novel Substituted Benzothiophene and ThienothiopheneCarboxanilides and Quinolones: Synthesis, Photochemical Synthesis, DNA-Binding Properties, Antitumor Evaluation and 3D-Derived QSAR Analysis. J Med Chem2012; 55: 5044-60.
24. Pongprom N,Bachitsch H,BauchingerA,Ettefagh H,Haider T, Hofer M,et al.Synthesis of new Benzo[*f*] isoindole-4,9-diones as anticancer compounds. Chem2010; 141: 53-62.
25. Smolarczyk R,Cichon T,Szala S Peptides: a new class of anticancer drugs. Posttepy High Med Dosw2009; 63: 360-368.
26. Landegren J,Borglund E,Storgårds K Treatment of scabies with disulfiram and benzyl benzoate emulsion: a controlled study. ActaDermVenereol 1979;59: 274–276.
27. Woerdenbag H,Windono T,Bos R,Riswan S,QuaxWJ Composition of the essential oils of *Kaempferia rotunda* L. and*Kaempferiaangustifolia* Roscoe rhizomes from Indonesia. Flavour Fragrance Jour 2004;19: 145–148.
28. Ferlay J, Shin HR, Bray F, Forman D, Mathers CD, Parkin D GLOBOCAN, Cancer Incidence and Mortality Worldwide: IARC Cancer Base No. 10. Lyon, France: International Agency for Research on Cancer 2008.
29. Bashyam MD Understanding cancer metastasis: an urgent need for using differential gene expression analysis. Cancer2002; 94: 1821–1829.
30. Madrid LV, Wang CY,Guttridge DC,Schottelius AJ, Baldwin AS Akt suppresses apoptosis by stimulating the transactivation potential of the RelA/p65 subunit of NF-kappaB. Mol Cell Biol2000; 20: 1626–1638.
31. Sliva D, Rizzo MT, English D Phosphatidylinositol 3-kinase and NF-kappaB regulate motility of invasive MDA-MB-231 human breast cancer cells by the secretion of urokinase-type plasminogen activator. J BiolChem2002; 277: 3150–3157.
32. Sheu J, Shih IM HLA-G and immune evasion in cancer cells. J Formosan Medical Ass Taiwan2010; 109: 248-257.

33. Szakács G, Paterson JK, Ludwig JA, Booth-Genthe C,Gottesman MM Targeting multidrug resistance in cancer. Nature Rev Drug Discov 2006; 5: 219-234.
34. Jana S,Mandlekar S Role of phase II drug metabolizing enzymes in cancer chemoprevention. Curr Drug Metab 2009; 10: 595-616.
35. Ono S, Yamakita Y, Yamashiro S, Matsudaira PT, Gnarra JR, Obinata T,et al. Identification of an actin binding region and a protein kinase C phosphorylation site on human fascin. J BiolChem1997: 272:2527–2533.
36. Moloney GP, Kelly DP, Mack P Synthesis of Acridine-based DNA Bis-intercalating Agents. Molecul 2001;6: 230-243.